THE ASTROPHYSICAL JOURNAL, 475:534–544, 1997 February 1

ESCAPE OF TeV GAMMA RAYS FROM ANISOTROPIC THERMAL PHOTON FIELDS IN ACTIVE GALACTIC NUCLEI

L. ZHANG AND K. S. CHENG
Department of Physics, University of Hong Kong, Pokfulam Road, Hong Kong
Received 1996 February 16; accepted 1996 August 20

ABSTRACT

We calculate the optical depth of TeV γ-rays that result from the anisotropic IR–UV thermal radiation of the α-disk model proposed by Shakura & Sunyaev. Our calculations yield the dependences of the optical depth of high-energy γ-rays on the disk parameters (i.e., α, M_8, and $\dot{M}_{26}$), photon energy, and Φ, the angle between the propagation direction and the rotation axis of the accretion disk. Our results indicate that TeV γ-rays can escape more easily from the central engine with lower values of α ($\lesssim 0.01$) and Φ. We conclude that the optical depth of TeV γ-rays in the anisotropic thermal radiation field places certain constraints on the possible values of the parameter α and the position of the emission region.

Subject headings: accretion, accretion disks — galaxies: active — gamma rays: theory

1. INTRODUCTION

Since MeV–GeV γ-rays emitted from many active galactic nuclei (AGNs) have been observed by EGRET (Fichtel et al. 1994; Thompson et al. 1995), the Whipple Observatory has made some observations in the TeV energy range for some AGNs (Kerrick et al. 1995a, 1995b). However, TeV γ-rays have been detected only from Mrk 421 (Punch et al. 1992) and Mrk 501 (Quinn et al. 1996). These observations raise questions about the origin of high-energy γ-rays and cosmic-ray particles from AGNs. In fact, if Mrk 421 and Mrk 501 are typical of AGNs, the particles responsible for the production of high-energy γ-rays should be accelerated to much higher than GeV energy. Why are these the only two TeV γ-ray AGN sources? A possible explanation is that a high-energy cutoff of γ-rays results from the absorption of high-energy γ-rays due to the pair production process $\gamma + \gamma \rightarrow e^{\pm}$, which can be divided into internal absorption inside the AGN and external absorption outside the AGN. The external absorption is due to the interaction of high-energy γ-rays with intergalactic infrared photons (see, e.g., Stecker, de Jager, & Salamon 1992; Stecker & de Jager 1993). Here we will focus on the internal absorption of very high energy γ-rays, especially near the central engine of an AGN.

High-energy particles (both protons and electrons) can be produced near the central engine of an AGN, which is believed to be a supermassive black hole accreting material from its environment (see, e.g., Rees 1984; Begelman, Blandford, & Rees 1984). An important physical quantity in the pair production process is the soft photon field around the central engine. The effect of pair production has been considered by many authors (e.g., Carraminana 1992; Bednarek 1993; Blandford 1993; Dermer & Schlickeiser 1993, 1994; Blandford & Levinson 1995; Becker & Kafatos 1995). In general, there are two varieties of the soft photon field. One is isotropic; it is dominated by scattered photons that are produced in the collisions of primary photons with diffuse gas or emission-line clouds. The optical depth of MeV–GeV γ-rays in this photon field has been calculated (Dermer & Schlickeiser 1993, 1994; Blandford & Levinson 1995), and the time- and energy-dependent optical depth of high-energy γ-rays up to TeV has also been calculated for this photon field (Bottcher & Dermer 1995). The other is anisotropic, which is emitted from the accretion disk. As a general consideration, Bednarek (1993) has estimated the optical depth of high-energy γ-rays in this photon field by using a simplified model. Recently, Becker & Kafatos (1995) estimated the absorption coefficient and optical depth of GeV γ-rays through an anisotropic X-ray photon field, where the X-ray field was assumed to be emitted in the inner region of a two-temperature accretion disk (see Shapiro, Lightman, & Eardley 1976). Having assumed a power-law distribution of the X-ray energy flux, Becker & Kafatos gave an analytic expression for the optical depth along the disk axis and predicted the focusing of γ-rays along the disk axis. For the absorption of very high energy γ-rays, the energy of soft photons is in the IR–UV region. Here we assume that the IR–UV photons are produced by the standard accretion disk proposed by Shakura & Sunyaev (1973, and references therein).

According to the theory of the standard accretion disk (Shakura & Sunyaev 1973), the disk will emit thermal photons whose distribution depends on the mass accretion rate, the mass of the black hole, a dimensionless coefficient α that parameterizes the frictional stress, and the disk structure. The distributions of surface temperature and local spectra of the thermal photons in different disk regions are different. In this paper, we make a more detailed investigation of the escape of high-energy γ-rays from the radiation field of the standard accretion disk. Section 2 presents the formulae that describe the thermal photon field from the accretion disk and the optical depth of the high-energy γ-rays due to pair production in the anisotropic thermal radiation field. In § 3, we calculate the optical depth of TeV γ-rays produced at the disk axis but propagating at an arbitrary angle with respect to this axis in the thermal radiation field produced by the disk, with several values of the mass accretion rate, mass of the black hole, and α. In § 4, a brief discussion is given.

2. THERMAL PHOTON FIELD AND OPTICAL DEPTH

For a quasi-Keplerian accretion disk around a black hole of mass M, the total radiation energy flux from the disk is always given by

$$Q(R) = \frac{3GM\dot{M}}{8\pi R^3}\left[1 - \left(\frac{6R_0}{10R}\right)^{1/2}\right] = 5.8 \times 10^{16} r^{-3} M_8^{-2} \dot{M}_{26}\left[1 - \left(\frac{0.6}{r}\right)^{1/2}\right] \text{ ergs cm}^{-2}\text{ s}^{-1}\,, \tag{1}$$

where M_8 is the black hole's mass in units of $10^8\ M_\odot$ and $\dot{M}_{26}$ is the mass accretion rate in units of 10^{26} g s^{-1}. The inner radius of the disk is at $6R_g$, and $R_g = GM/c^2 = 1.5 \times 10^{13} M_8$ cm is the Schwarzschild radius of the black hole. Hereafter, the distances involved in this paper are expressed in units of $R_0 = 10R_g$, e.g., $r = R/R_0$.

In the standard accretion disk (Shakura & Sunyaev 1973), the disk is divided into three regions—inner, intermediate, and outer—and each region has its own equations of structure. If the energy flux in each region is represented by I_i, where $i = 1, 2$, and 3 label inner, intermediate, and outer, respectively, then from equation (1) the energy flux of soft photons with energy E can be easily read as

$$I_i = \frac{Q(r)}{2\pi C_i kT_i} F_i(X_i)\,, \tag{2}$$

where k is Boltzmann's constant, $X_i = E/kT_i$, $C_i = \int_0^\infty F_i(X_i)dX_i$, and $F_i(X_i)$ is the normalized radiation spectrum. According to Shakura & Sunyaev (1973), the surface temperatures (T_i) and $F_i(X_i)$ at different disk regions can be easily obtained as follows:

Inner region.—In this region, the expression for the surface temperature depends on the opacity in the disk, τ^*, which is given by

$$\tau^* = 6.5 \times 10^{-4} \alpha^{-17/16} M_8^{-31/16} \dot{M}_{26}^{-2} r^{57/16} [1 - (0.6/r)^{1/2}]^{-2}\,. \tag{3}$$

The surface temperature is

$$T_1 = \begin{cases} 9.1 \times 10^{10} \alpha^{2.4} M_8^{-4.8} \dot{M}_{26}^{4.8} r^{-7.2} [1 - (0.6/r)^{1/2}]^{4.8}\ \text{K}\,, & \text{for } \tau^* < 1\,, \\ 3.4 \times 10^{6} \alpha^{0.2} M_8^{-1} \dot{M}_{26}^{0.8} r^{-1.5} [1 - (0.6/r)^{1/2}]^{0.8}\ \text{K}\,, & \text{for } \tau^* > 1\,. \end{cases} \tag{4}$$

The normalized radiation spectrum is

$$F_1(X_1) = X_1^3 \exp(-X_1)\,, \tag{5}$$

and $C_1 = \int_0^\infty F(X_1)dX_1 = 6$.

Intermediate region.—In this region, there are two kinds of atmospheric structure: homogeneous and exponentially varying. For the homogeneous atmosphere, the surface temperature and $F_2(X_2)$ are

$$T_2 = 5.4 \times 10^6 \alpha^{2/9} M_8^{-10/9} \dot{M}_{26}^{8/9} r^{-5/3}\left[1 - \left(\frac{0.6}{r}\right)^{1/2}\right]^{28/75} \text{K}\,, \qquad F_2(X) = \frac{X_2^{3/2} \exp(-X_2)}{[1 - \exp(-X_2)]^{1/2}}\,, \tag{6}$$

respectively, where $C_2 \approx 1.5$. For the exponentially varying atmosphere,

$$T_2 = 4.5 \times 10^5 \alpha^{1/75} M_8^{-47/75} \dot{M}_{26}^{28/75} r^{-141/151}\left[1 - \left(\frac{0.6}{r}\right)^{1/2}\right]^{28/75} \text{K}\,, \qquad F_2(X) = \frac{X_2^2 \exp(-X_2)}{[1 - \exp(-X_2)]^{1/3}}\,, \tag{7}$$

and $C_3 \approx 2.1$.

Outer region.—The surface temperature in this region is

$$T_3 = 1.0 \times 10^5 M_8^{-2/3} \dot{M}_{26}^{2/3} r^{-3/4} [1 - (0.6/r)^{1/2}]^{1/4}\ \text{K}\,, \tag{8}$$

where $F_3(X_3) = X_3^3 \exp(-X_3)$ and $C_3 \approx 6.5$.

In our calculations, the surface temperature varying with the radius of the disk is calculated first. In the intermediate region, either the exponential or the homogeneous atmosphere is used, so that the surface temperature varies smoothly with disk radius. The thermal radiation from the disk has a peak in the IR–UV range, depending on the surface temperature of the disk. From the above expressions, the spectral distribution of the radiation from the whole disk observed at a position very far from the disk is obtained by integrating the local spectrum:

$$F_\nu = 3.3 \times 10^{35} \dot{M}_{26} \sum_i \int \frac{F_i(X_i)}{C_i} \frac{r^{-3}[1 - (0.6/r)^{1/2}]}{T_i(r)}\, r\, dr \text{ ergs}^{-1}\text{ Hz}^{-1}\,. \tag{9}$$

From equation (9), the spectral distribution of the radiation depends on α, M_8, and $\dot{M}_{26}$.

Now we consider the optical depth of high-energy γ-rays. Let us assume that γ-rays of energy E_γ are produced at disk radius r_p and height z_p (where r_p and z_p are in units of R_0) above the disk and propagate at an angle Φ with respect to the z-axis. The γ-rays interact with soft photons at a point p, which is close to the disk (see Fig. 1). If the interaction angle between photons is Θ, then the differential optical depth is

$$d\tau_{\gamma\gamma}^i = \frac{I_i}{cE} \sigma_{\gamma\gamma}(v)(1 - \cos\Theta) \frac{\rho \cos\theta}{S^3}\, r\, dr\, dE\, d\phi\, d\lambda\,. \tag{10}$$

In equation (10), $\sigma_{\gamma\gamma}$ is the cross section of pair production, which is expressed by

$$\sigma(E, E_\gamma) = \frac{3\sigma_T}{16}(1 - v^2)\left[(3 - v^4)\ln\left(\frac{1+v}{1-v}\right) - 2v(2 - v^2)\right], \tag{11}$$

where σ_T is the Thomson cross section and v is determined by using the relation $1 - v^2 = 2m_e^2 c^4/(1 - \mu)E_\gamma E$, where $\mu = \cos \Theta$. S is the distance between the photon-photon interaction point and the soft photon emission point in the disk, in units of R_0. In spherical coordinates (ρ, θ, ϕ), S can be represented as

$$S^2 = \rho^2 + r^2 - 2\rho r \sin\theta \cos\phi\ . \tag{12}$$

From the geometry, the distance traversed by a high-energy γ-ray since its creation and the interaction angle can be expressed as

$$\lambda^2 = (\rho \sin\theta - r_p)^2 + (\rho \cos\theta - z_p)^2\ , \qquad \cos\Theta = S^{-1}[(z_p \cos\theta + \lambda) - r\cos\phi \sin\Phi]\ . \tag{13}$$

Therefore the optical depth of γ-rays for the soft photons emitted from each region of the disk is given by

$$\tau^i_{\gamma\gamma}(r_p, z_p, \Phi, E_\gamma) = \int_0^\infty \int_{E_{\min}(\Theta)}^\infty \int_0^{2\pi} \int_{r_{i-1}}^{r_i} \frac{I_i}{cE}\, \sigma_{\gamma\gamma}(\beta)\, \frac{\rho\cos\theta}{S^3}\, r\, dr\, dE\, d\phi\, d\lambda\ , \tag{14}$$

where $i = 1$, 2, or 3, representing inner, intermediate, and outer regions of the disk, respectively. The total optical depth is the sum of the individual optical depths. Introducing the variable y, defined by

$$y^{-1} = \lambda + z_p \cos\Phi + r_p \sin\Phi\ , \tag{15}$$

equation (14) becomes

$$\tau^i_{\gamma\gamma}(z_p, r_p, \Phi, E_\gamma) = \int_0^{(z_p\cos\Phi + r_p\sin\Phi)^{-1}} \int_0^1 \int_{r_{i-1}}^{r_i} \int_0^{2\pi} I_i(1 - \cos\Theta)\sigma(v)\, \frac{2v}{1 - v^2}\, \frac{z_p y \sin^2\Phi + \cos\Phi - r_p y \sin\phi\cos\phi}{(yS)^3}\, r\, dr\, d\phi\, dv\, dy\ , \tag{16}$$

where S and $\cos\Theta$ are given by

$$S = \frac{1}{y}\left\{1 + [(z_p \sin\Phi)^2 + r^2 + (r_p\cos\Phi)^2]y^2 - 2ry\left[1 - y\left(z_p\cos\Phi + r_p\sin\Phi - z_p\frac{r_p}{r} - r_p\csc\Phi\right)\right]\sin\Phi\cos\phi\right\}^{1/2}\ , \tag{17}$$

$$\cos\Theta = \frac{1}{yS}(1 - yr\cos\phi\sin\Phi)\ . \tag{18}$$

Equation (16) is the general expression for the optical depth of γ-rays for the soft photons emitted from each region of the disk. The propagation direction of a high-energy γ-ray emitted at the point (r_p, z_p) is specified by the angle Φ. For a γ-ray

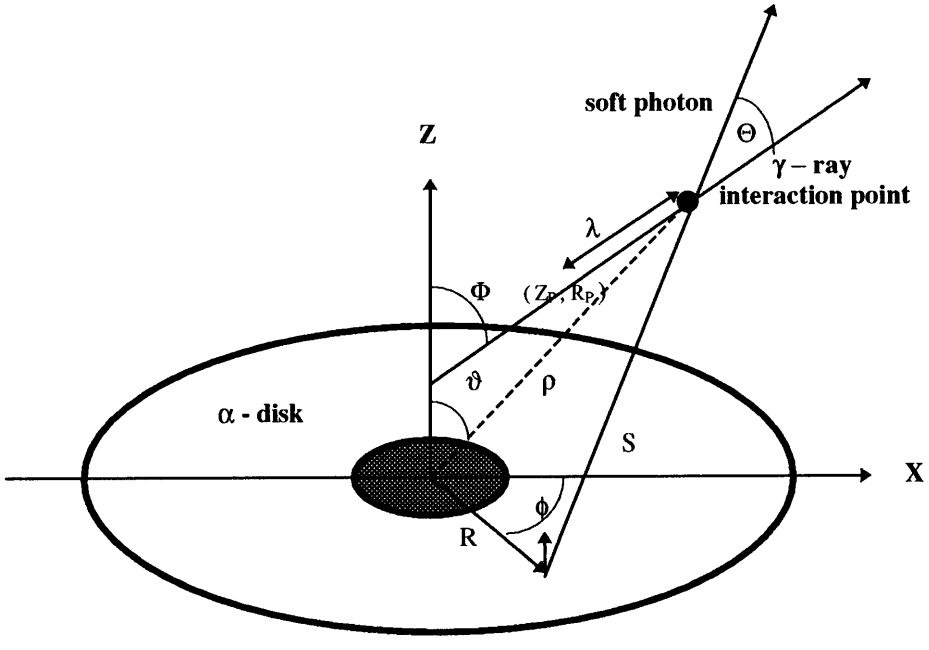

FIG. 1.—Schematic diagram of γ-ray propagation above a thin, α accretion disk surrounding a supermassive black hole

produced at the disk axis ($r_p = 0$) and propagating along the z-axis (i.e., $\Phi = 0$), equation (16) for the γ-ray optical depth can be simplified to

$$\tau^i_{\gamma\gamma}(z_p, E_\gamma) = 2\pi \int_0^{z_p^{-1}} \int_0^1 \int_{r_{i-1}}^{r_i} I_i\{1 - [1 + (rt)^2]^{-0.5}\}\sigma(v)[1 + (rt)^2]^{-3/2} \frac{2v}{1 - v^2} r\, dr\, dv\, dt\ , \tag{19}$$

where $t^{-1} = \lambda + z_p$. On the other hand, if high-energy γ-rays are emitted at the disk axis but propagate at an arbitrary angle Φ with respect to the this axis, then the optical depth can be written

$$\tau^i_{\gamma\gamma}(z_p, \Phi, E_\gamma) = \int_0^{(z_p \cos \Phi)^{-1}} \int_0^1 \int_{r_{i-1}}^{r_i} \int_0^{2\pi} I_i(1 - \cos \Theta)\sigma(v) \frac{2v}{1 - v^2} \frac{z_p u \sin^2 \Phi + \cos \Phi}{(uS)^3} r\, dr\, d\phi\, dv\, du\ , \tag{20}$$

where S is given by equation (17) with $r_p = 0$, $\cos \Theta = (1 - ru \cos \phi \sin \Phi)/uS$, and $u^{-1} = \lambda + z_p \cos \Phi$. For given values of α, M_8, and $\dot{M}_{26}$, the total optical depth of high-energy γ-rays at a certain position can be obtained from

$$\tau_{\gamma\gamma} = \sum_{i=1}^{3} \tau^i_{\gamma\gamma}. \tag{21}$$

3. ASYMPTOTIC BEHAVIOR OF THE OPTICAL DEPTH

It appears that $(L/L_E)/(Z_p/10R_g)$ may be regarded as a basic scaling factor, where it is assumed that the cross section of pair production of γ-rays is independent of energy and that photon density depends only on L and $1/z_p^2$. However, in the system in which we are interested, the exact characteristic energy is kT_s, so both photon density and the cross section are energy dependent. We present a more detailed analysis of the asymptotic behavior of the optical depth of high-energy γ-rays in this section. Here we consider the case of γ-rays propagating along the disk axis. In this case, it is possible to give an asymptotic expression for the optical depth after some simplifications. The M_8 and $\dot{M}_{26}$ in different disk regions are different, so it is difficult to obtain an analytic approximation. In order to determine the asymptotic behavior of the optical depth, the following assumptions are made: (1) a single distribution of the disk photons is used instead of the different distributions for different disk regions; (2) the pair production cross section for the high-energy γ-rays has the form

$$\sigma_{\gamma\gamma} \sim \frac{3}{2} \sigma_T \frac{1}{s}(1 + 4s)(\ln s - 1) \tag{22}$$

(Gould & Schréder 1967), where $s = 2EE_\gamma(1 - \cos \Theta)/(m_e c^2)^2$; (3) for a given γ-ray energy, only disk photons with energies $E > E_{th}$ contribute to the pair production of the γ-rays, where $E_{th} = m_e^2 c^4/E_\gamma$. Thus we can define a radius, $\bar{r}$, of the disk by using $\langle kT_s \rangle \approx E_{th}$ such that the disk photons produced within the radius $\bar{r}$ can be responsible for the pair production of γ-rays with energy E_γ. Note that $\bar{r}$ depends on E_γ, M_8, and $\dot{M}_{26}$. For the exponential distribution of disk photons, $\bar{r} \sim 200$ for $E_\gamma = 1$ TeV. Furthermore, we assume that $\cos \Theta \to 1$, which means $rt \ll 1$ and $\cos \Theta \sim 1 - r^2t^2/2$ in equation (19). From the limits of the integral over t, we know that the condition $rt \ll 1$ is valid if $\bar{r}/z_p \leq 1$. Under the above assumptions, we use the exponential distribution for the disk photons because of its importance in the intermediate region. We approximate the integral over r as the product of $\bar{r}$ and the integrated function with $r = \bar{r}$ in equation (19) at first and then integrate equation (19) over s, with $2v\, dv/(1 - v^2) = -ds/s$. Finally, we calculate the integral over t. For this, we replace $r^{-14/15}$ by r^{-1} and assume that $t\bar{r} \sim 1.5$ to give the analytic form of the optical depth. Therefore the optical depth in the case of $\cos \Theta \to 1$ can be approximated as

$$\tau_{\gamma\gamma} \sim 10^5 \frac{\dot{M}_{26}}{M_8} f \frac{1}{z_p} \exp(-6A_0 f z_p)\ , \tag{23}$$

where $f = (M_8/\dot{M}_{26})^{47/75}\dot{M}_{26}^{19/75}$ and $A_0 = (m_e c^2)^2/(E_\gamma kT_0) \approx 6/E_\gamma$ (GeV). In deriving equation (23), the expressions of T_s and $F(X)$ for the exponential atmosphere have been used. From this expression, it can be seen that the optical depth drops exponentially with z_p at large distances from the black hole and varies with M_8 and $\dot{M}_{26}$. On the other hand, for the case of $\cos \Theta \to 0$, we have that $\tau_{\gamma\gamma} \propto z_p^2$. For a blackbody distribution of photon density [i.e., $F(X) = X^3 \exp(-X)$], the asymptotic behavior of the optical depth is proportional to $\exp(-6A_0 z_p)/z_p$, with $A_0 \sim 30/E_\gamma$ (GeV). Although this analytic approximation is not good for $Z_p/10R_g < 10$, this formula is still very useful because it is unlikely that γ-ray production will occur very close to the black hole.

4. MODEL RESULTS

In order to carry out the numerical calculation, we need to specify the three parameters M_8, $\dot{M}_{26}$, and α first, which describe the disk properties such as surface temperature, total energy flux, and thermal photon density. Generally, the range of α-values is from 10^{-3} to 1 because there is no consensus on the viscous processes in the accretion disk. For M_8 and $\dot{M}_{26}$, two assumptions, which relate M_8 and $\dot{M}_{26}$ to the luminosity, are used. First, the total radiation power is taken to equal the accretion power. From equation (1), the integrated disk luminosity is then given by

$$L_{disk} = \int_{0.6}^{\infty} Q 2\pi r\, dr \approx 6.7 \times 10^{45} \dot{M}_{26}\ \text{ergs}^{-1}\ . \tag{24}$$

Second, the observed luminosity is assumed to be less than or equal to the Eddington luminosity, that is,

$$L_{\rm E} \leq 4\pi GMm_p c/\sigma_{\rm T} \approx 1.3 \times 10^{46} M_8 \ {\rm ergs}^{-1} \ . \tag{25}$$

Using the relation $L_{\rm disk} \leq L_{\rm E}$, we have $\dot{M}_{26} \leq 1.9 M_8$ (we define $\dot{M}_{26}^{\rm E} = 1.9 M_8$). In fact, the values of M_8 and $\dot{M}_{26}$ for a specific AGN have not been determined definitely. Therefore a wide range of M_8, from 0.1 to 100, is taken for our calculations. For a given M_8, the values of $\dot{M}_{26}$ and α can be adjusted so that the luminosity satisfies the observed features (e.g., the position of the IR–UV bump). Thus the optical depth of high-energy γ-rays for a given energy E_γ due to pair production can be calculated. Here we will focus on the optical depth of TeV γ-rays.

In our calculations, the surface temperatures of the disk versus r are calculated for different values of α, M_8, and $\dot{M}_{26}$ at first. In Figure 2*a*, the surface temperatures for several values of α and $M_8 = \dot{M}_{26} = 1$ are shown; Figure 2*b* shows the surface temperatures for $\alpha = 0.01$, $M_8 = 1$, and $\dot{M}_{26} = 0.1\dot{M}_{26}^{\rm E}$, $0.3\dot{M}_{26}^{\rm E}$, and $\dot{M}_{26}^{\rm E}$. From Figure 2, it can be seen that different values of α have a significant influence on the surface temperature in the inner region of the disk (Fig. 2*a*) and that changing $\dot{M}_{26}$ shifts the surface temperature over the whole disk (Fig. 2*b*). On the other hand, the surface temperatures for a given α have the same shape but different values when M_8 and $\dot{M}_{26}$ are changed simultaneously. Next the disk luminosity is calculated. For example, the luminosities emitted from the three disk regions and the total luminosity from the whole disk for $\alpha = 0.01$, $M_8 = 1$, and $\dot{M}_{26} = 1$ are shown in Figure 3*a*. In Figure 3*b*, the disk luminosities for $\alpha = 0.01$, $M_8 = 0.1$, and $\dot{M}_{26} = 0.1\dot{M}_{26}^{\rm E}$,

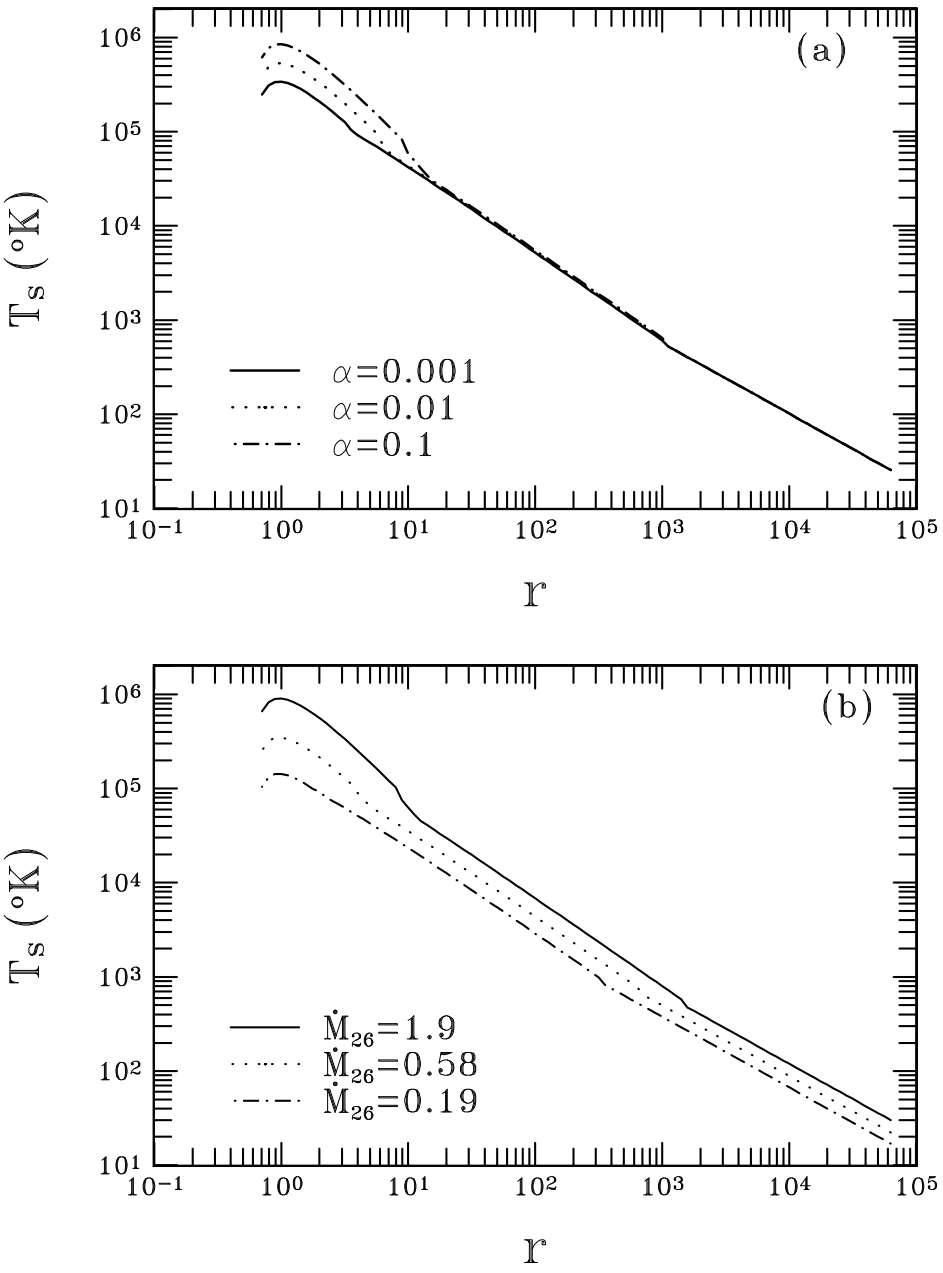

FIG. 2.—Surface temperature of the α-disk vs. disk radius for (*a*) $M_8 = 1$, $\dot{M}_{26} = 1$, and $\alpha = 0.001$, 0.01, and 0.1 and for (*b*) $\alpha = 0.01$, $M_8 = 1$, and $\dot{M}_{26} = 1.9$, 0.58, and 0.19.

$0.3\dot{M}_{26}^{E}$, and $\dot{M}_{26}^{E}$ are illustrated. It can be seen that the luminosities from the inner, intermediate, and outer parts of the disk make their main contributions to the low-, middle-, and high-frequency regions of the total luminosity, respectively (see Fig. 3*a*), and that the total luminosity of the disk for given α and M_8 varies with $\dot{M}_{26}$.

Furthermore, we consider in detail the case of TeV γ-rays propagating along the disk axis, where the TeV γ-rays are produced at a height z_p above the center of the disk. The optical depth of γ-rays can be calculated by using equations (19) and (21). First, in order to understand the effect of different α-values on the optical depth of TeV γ-rays, the optical depths of γ-rays of energy $E_\gamma = 1$ TeV with changing α have been calculated for given values of M_8, $\dot{M}_{26}$, and z_p, and the results are shown in Figure 4. It can be seen from this figure that the optical depth increases with increasing α and changes more rapidly for higher values of M_8 and $\dot{M}_{26}$ as compared with lower values of M_8 and $\dot{M}_{26}$. It seems that a lower α allows TeV γ-rays to escape from the central engine more easily. Second, the optical depths of γ-rays of energy $E_\gamma = 1$ TeV varying with height z_p have been calculated in this case and are shown in Figure 5, where $\alpha = 0.01$ and different values of M_8 and $\dot{M}_{26}$ are adopted. In this figure, the scaling factor, $(L/L_E)/(Z_p/10R_g)$, has been used. The feature of $\tau_{\gamma\gamma}$ versus z_p is to increase with z_p at first and to exponentially drop at large z_p, which is the same as the asymptotic behavior described in § 3. As examples, the asymptotic results obtained from equation (23) for different M_8 and $\dot{M}_{26}$ are shown in this figure. From Figure 5, note that there are some differences for different M_8 and $\dot{M}_{26}$ due to the dependence of $F_i(X_i)$ on M_8 and $\dot{M}_{26}$. From the asymptotic expression, these differences at large z_p are due to the dependence of the exponential term on M_8 and $\dot{M}_{26}$. Obviously, the optical depth increases markedly when moving toward the central engine, and TeV γ-rays close to the black hole cannot escape from the

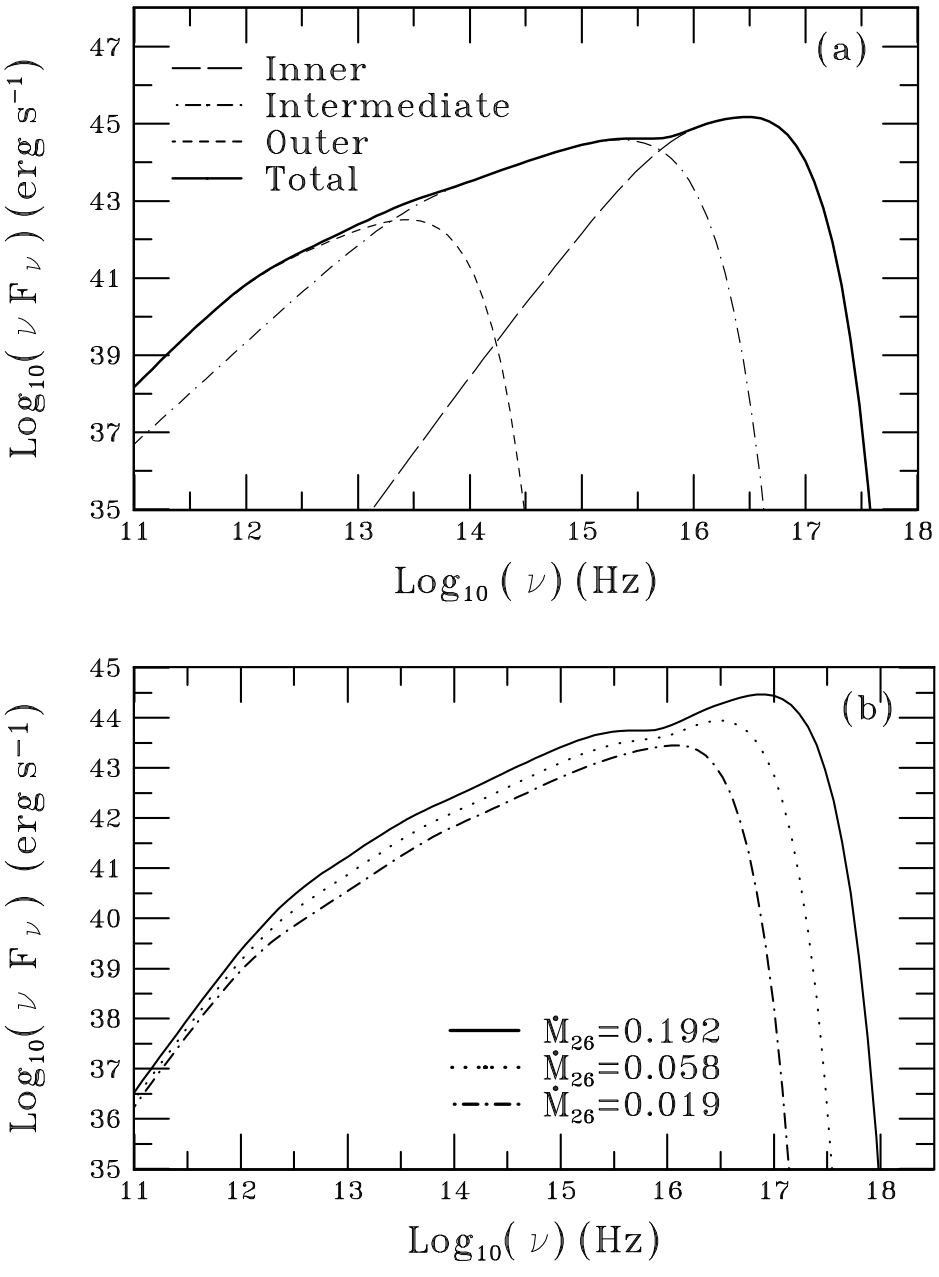

FIG. 3.—Disk luminosity vs. frequency for (*a*) $\alpha = 0.01, M_8 = 1$, and $\dot{M}_{26} = 1$ and for (*b*) $\alpha = 0.01, M_8 = 0.1$, and $\dot{M}_{26} = 0.192, 0.058$, and 0.019

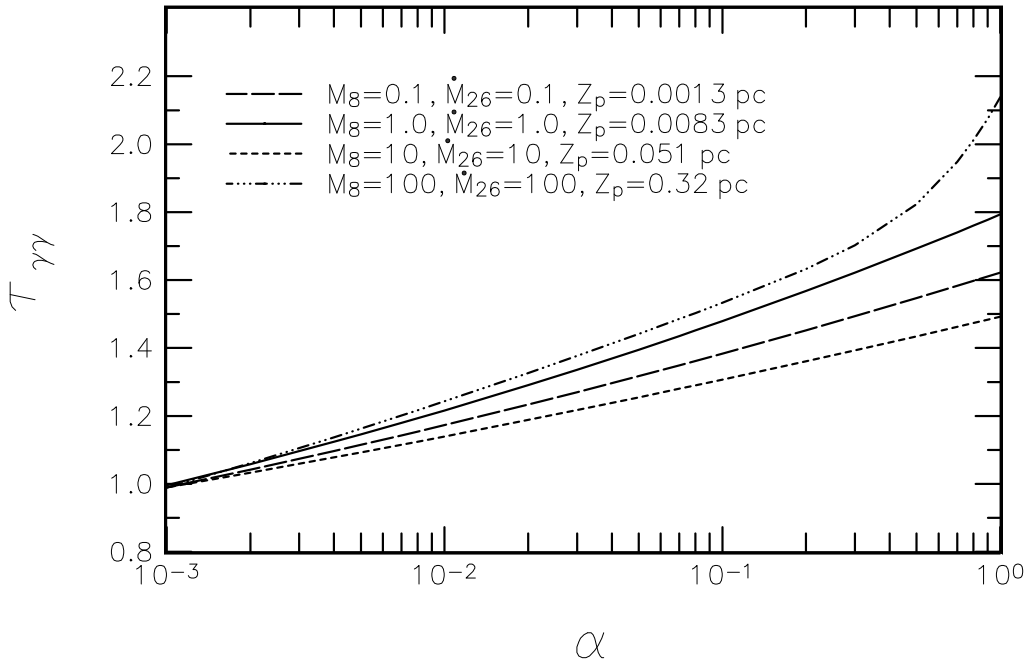

FIG. 4.—Optical depth of TeV γ-rays propagating along the disk axis as a function of α for given M_8, $\dot{M}_{26}$, and z_p

source, as a result of higher opacity. Third, the optical depths of very high energy γ-rays versus energy for $M_8 = 1.0$ and $\dot{M}_{26} = 1.92$, 0.58, and 0.19 are shown in Figure 6; the results indicate that the optical depth of γ-rays increases more rapidly with energy in the lower energy region as compared to that in the higher energy region, and the optical depth for lower values of $\dot{M}_{26}$ is less than that for higher values of $\dot{M}_{26}$.

It is important to investigate the angular dependence of optical depth. Here we assume that TeV γ-rays are created at a point of $z = z_p$ and $r_p = 0$ above the disk and propagate at an angle Φ with respect to the disk axis. The optical depth can be calculated by using equations (20) and (21) for fixed values of M_8, $\dot{M}_{26}$, α, z_p, and E_γ. In Figure 7, the dependence of optical depth with $\alpha = 10^{-3}$, 10^{-2}, 0.1, and 1 on propagation angle Φ for $M_8 = 1$, $\dot{M}_{26} = 1$, $Z_p\,(=R_0\,z_p) = 0.01$ pc, and $E = 1$ TeV is shown. The main feature is that TeV γ-rays can escape easily from the central engine in regions of smaller Φ above a certain z_p and that this angular region becomes wider for larger values of α. For fixed α, M_8, E, and Z_p, changing $\dot{M}_{26}$ (which is limited by the relation of M_8 and $\dot{M}_{26}$) has an important effect on the optical depth of γ-rays; the results for $\alpha = 0.01$, $E_\gamma = 1$ TeV,

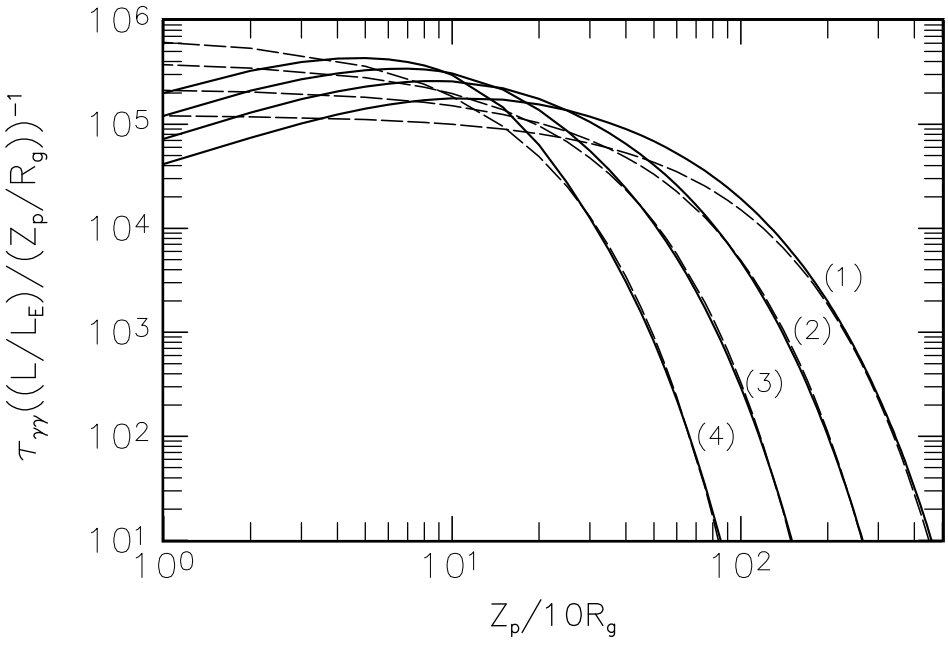

FIG. 5.—Numerical (*solid lines*) and asymptotic (*dashed lines*) optical depths of TeV γ-rays propagating along the disk axis as functions of the distance to the black hole, with $\alpha = 0.01$, $E_\gamma = 1$ TeV, and several M_8 and $\dot{M}_{26}$: (1) $M_8 = 0.1$ and $\dot{M}_{26} = 0.1$, (2) $M_8 = 1$ and $\dot{M}_{26} = 1$, (3) $M_8 = 10$ and $\dot{M}_{26} = 10$, and (4) $M_8 = 100$ and $\dot{M}_{26} = 100$.

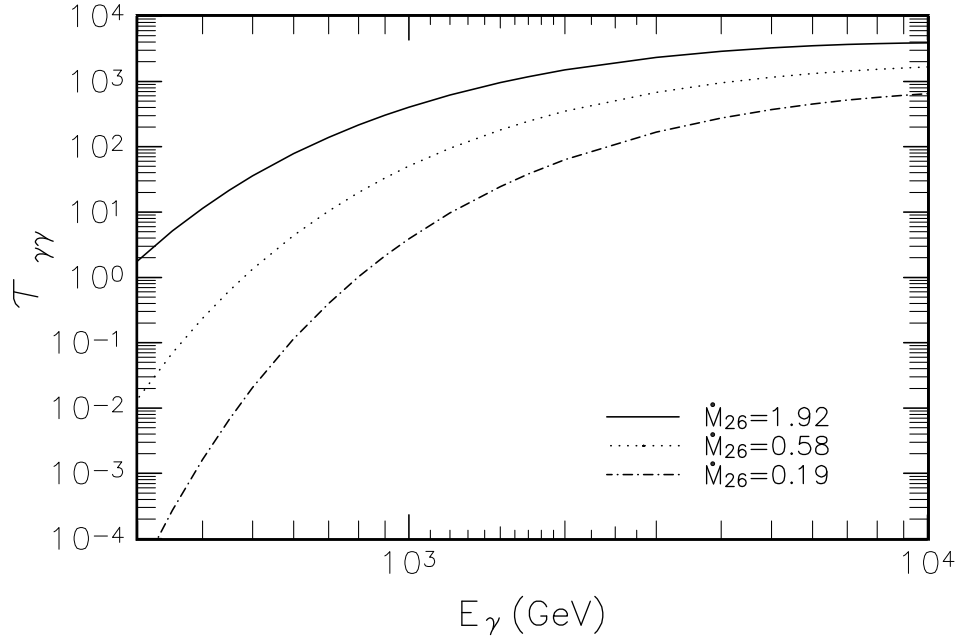

FIG. 6.—Optical depth of very high energy γ-rays at $Z_p = 10^{16}$ cm propagating along the disk axis as a function of energy for $\alpha = 0.01$, $M_8 = 1$, and $\dot{M}_{26} = 1.92, 0.58$, and 0.19.

$Z_p = 10^{16}$ cm, $M_8 = 0.3$, and $\dot{M}_{26} = \dot{M}_{26}^{\rm E}$, $0.3\dot{M}_{26}^{\rm E}$, and $0.1\dot{M}_{26}^{\rm E}$ are shown in Figure 8. To understand the effect of different values of M_8 and $\dot{M}_{26}$ on the angular dependence of optical depth, the calculated results of the optical depth with two different values of M_8 and $\dot{M}_{26}$ (where $\dot{M}_{26} = 0.3\dot{M}_{26}^{\rm E}$ is adopted) are shown in Figure 9, where $\alpha = 0.01$ and $Z_p = 10^{17}$ cm. It can be seen from Figure 9 that the optical depths for different M_8 and $\dot{M}_{26}$ in the region of small Φ are much less than those in the region of larger Φ. Finally, the optical depths at $Z_p = 3 \times 10^{15}$, 5×10^{15}, and 10^{16} cm for $\alpha = 0.01, E_\gamma = 1$ TeV, $M_8 = 0.1$, and $\dot{M}_{26} = 0.3M_{26}^{\rm E}$ are shown in Figure 10. From Figures 7–10, we can conclude that there is strong focusing of the escaping TeV γ-rays along the disk axis.

It is also interesting to estimate the distance to the TeV γ-ray emission site, $z_{\gamma\gamma}$, which is determined by $\tau_{\gamma\gamma} = 1$. As mentioned above, the optical depth of TeV γ-rays propagating along the disk axis has a minimum value, so we estimate the distance in the case of γ-rays propagating along the disk axis. In Table 1, the distances for different M_8 and $\dot{M}_{26}$ are listed, where $\alpha = 0.01$ and $M_8 = \dot{M}_{26}$ are adopted. If the timescale in which light crosses the distance $z_{\gamma\gamma}$ is $t_{\rm var}$, then, using the relation $t_{\rm var} = Z_{\gamma\gamma}/c$, where c is the speed of light and $Z_{\gamma\gamma} = z_{\gamma\gamma}R_0$, we can estimate the time variability, and the values so

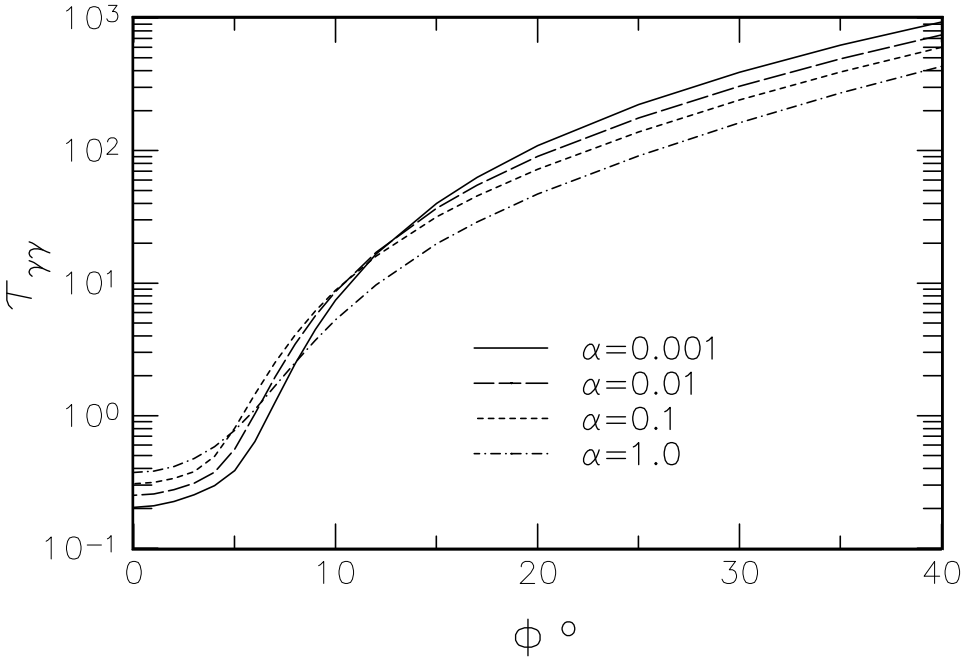

FIG. 7.—Angular dependence of the optical depth of TeV γ-rays for different values of α. The other parameters are $M_8 = 1$, $\dot{M}_{26} = 1$, and $Z_p = 0.01$ pc

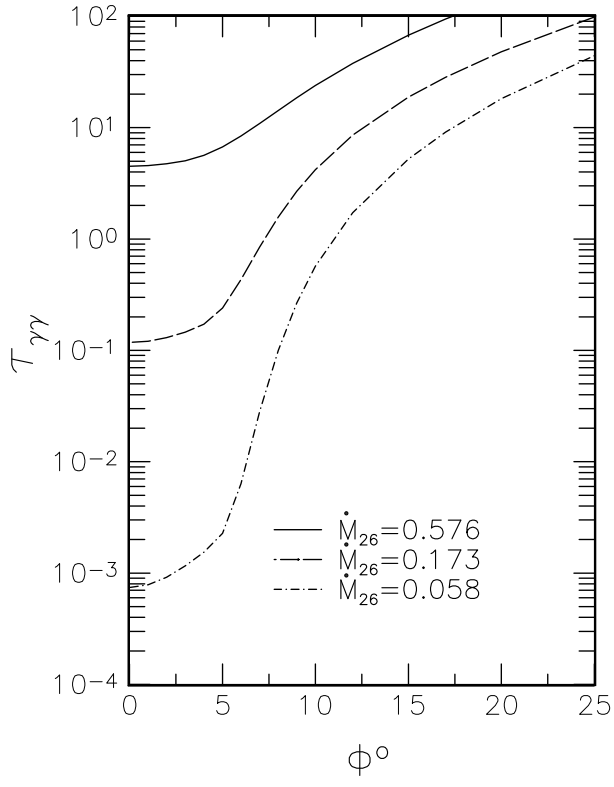

FIG. 8.—Optical depth of γ-rays with $E_\gamma = 1$ TeV vs. angle Φ at $Z_p = 10^{17}$ cm for $\alpha = 0.01$, $M_8 = 0.3$, and $\dot{M}_{26} =$ 0.58, 0.17, and 0.058

obtained are also listed in Table 1. Obviously, lower values of M_8 and $\dot{M}_{26}$ correspond to lower values of $z_{\gamma\gamma}$ and thus $t_{\rm var}$, which indicates that the distance to the γ-ray emission site for a specific AGN with lower luminosity is close to the central engine; for example, the distance for $M_8 = 0.1$ and $\dot{M}_{26} = 0.1$, for which the corresponding luminosity is $\sim 10^{45}$ ergs s^{-1}, is $\sim 1.3 \times 10^{-3}$ pc. As another example, we consider 3C 279: the possible value of M_8 is ~ 10 (Becker & Kafatos 1995), so we have $Z_{\gamma\gamma} \approx 5.2 \times 10^{-2}$ pc and $t_{\rm var} \approx 60$ days. After dividing our result by a factor of $1 + z$ (where z is redshift), the result is

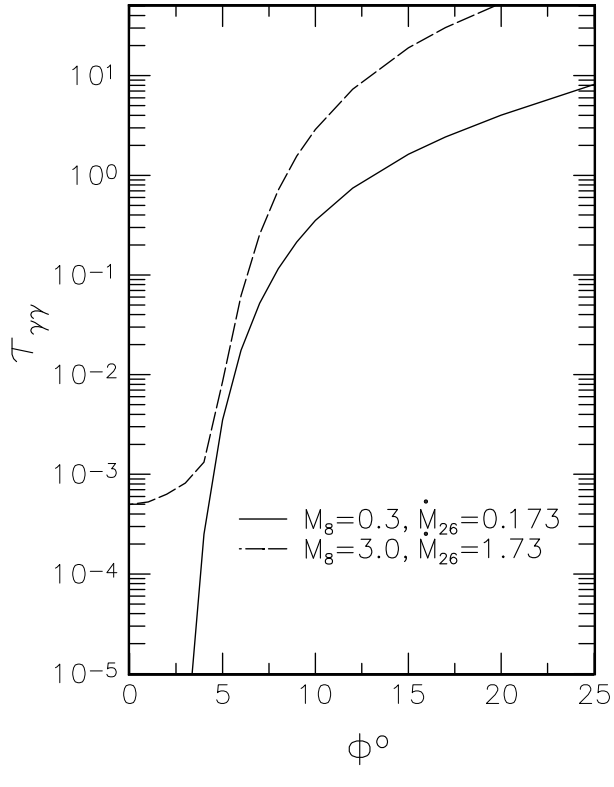

FIG. 9.—Angular dependence of the optical depth of γ-rays for different values of M_8 and $\dot{M}_{26}$, where $\alpha = 0.01$, $E_\gamma = 1$ TeV, and $Z_p = 10^{16}$ cm

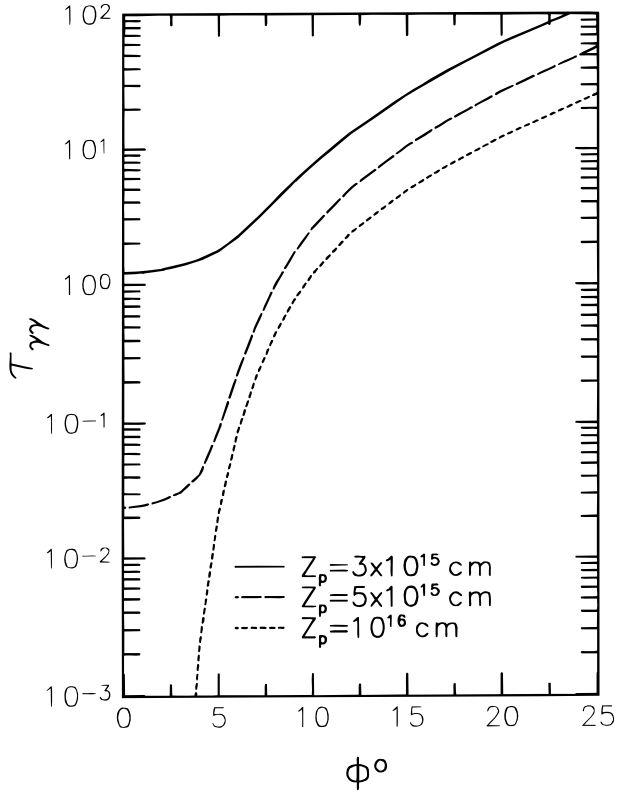

FIG. 10.—Optical depths of γ-rays at $Z_p = 5 \times 10^{15}$, 5×10^{15}, and 10^{16} cm for $\alpha = 0.01$, $E_\gamma = 1$ TeV, $M_8 = 0.1$, and $\dot{M}_{26} = 0.58$

TABLE 1

DISTANCES TO EMISSION SITES

M_8, $\dot{M}_{26}$	$Z_{\gamma\gamma}$ (pc)	$t_{\rm var}$ (days)
0.1	1.3×10^{-3}	1.5
0.5	4.8×10^{-3}	5.6
1.0	8.4×10^{-3}	9.7
5.0	3.0×10^{-2}	34.7
10.0	5.2×10^{-2}	60.2
20.0	9.0×10^{-2}	104.2
50.0	1.9×10^{-1}	216.0
70.0	2.4×10^{-1}	283.2
100.0.....	3.2×10^{-1}	37460

NOTE.—The distances to TeV γ-ray emission sites for $\alpha = 0.01$ and different values of M_8 and $\dot{M}_{26}$, which are determined by $\tau_{\gamma\gamma} = 1$. Corresponding timescales of variability are calculated by using $t_{\rm var} = Z_{\gamma\gamma}/c$.

much higher compared with the observed variability timescale of 3C 279 in the EGRET energy region ($t_{\rm var} \approx 2$ days; von Montigny et al. 1995). If this is true, our result indicates that the emission region of TeV γ-rays is different from that of GeV γ-rays in 3C 279.

5. DISCUSSION

As an important process, the absorption of high-energy γ-rays due to pair production in collisions with thermal photons emitted by the standard accretion disk can prevent the free escape of high-energy γ-rays with certain energies produced in the central engine of an AGN, depending on the parameters, α, M_8, and $\dot{M}_{26}$, of the accretion disk. In fact, the importance of the absorption effects should be in the more energetic part of the γ-ray spectrum for AGNs because of the lower characteristic temperatures of disks around massive black holes.

Our calculation results for the optical depth of TeV γ-rays due to pair production imply that the optical depth at a given distance from the central engine depends mainly on the parameters of the standard disk, i.e., M_8, $\dot{M}_{26}$, and α. Although the range of α is very uncertain, our expected optical depth of TeV γ-rays along the disk axis increases with α for given M_8 and $\dot{M}_{26}$ (see Fig. 4), so the γ-rays can escape from the central engine more easily in disks with smaller values of α. On the other hand, from Figure 7, the angular region where TeV γ-rays can escape is wider in disks of smaller α for fixed M_8, $\dot{M}_{26}$, and z_p.

Therefore we conclude that, for the central engines of disks with smaller values of α, TeV γ-rays can escape more easily and the possible range of α is between 0.001 and 0.01. For the dependence of the optical depth of high-energy γ-rays on M_8 and $\dot{M}_{26}$, the optical depth for lower values of M_8 and $\dot{M}_{26}$ is less than that for higher values of M_8 and $\dot{M}_{26}$. As for the angular dependence of the optical depth of TeV γ-rays, our calculation results indicate that TeV γ-rays escape preferentially from the central engine along the disk axis. For example, the half-width of the angular distribution, $\Delta\Phi$, of the optical depth at $Z_p = 5 \times 10^{15}$ cm for $\alpha = 0.01$, $M_8 = 0.1$, and $\dot{M}_{26} = 0.3\dot{M}_{26}^{E}$ is $\sim 7°$.

The recent survey of TeV γ-ray emission from AGNs by the Whipple Observatory only found two TeV γ-ray sources, namely, Mrk 421 and Mrk 501, out of 36 sources, and the observations of Mrk 421 and Mrk 501 indicate TeV γ-ray flares with a variability timescale of 2 days (Kerrick et al. 1995a, 1995b; Macomb et al. 1995; Quinn et al. 1996). This variability timescale corresponds to a light-crossing distance of 5×10^{15} cm. The current explanation is that the intergalactic IR can absorb TeV γ-rays from sources at distances greater than $\approx 614\, h_0^{-1}$ Mpc (i.e., the corresponding redshift is ~ 0.1; Stecker et al. 1992), where h_0 is the Hubble constant in units of 50 km s^{-1} Mpc^{-1}. However, there are still 15 nearby sources for which the range of redshifts is from 0.003 to 0.069 (Kerrick et al. 1995a, 1995b). In our model, there are two factors to affect the detection of TeV γ-ray sources. First, the intrinsic IR–UV luminosity must be lower than $\approx 10^{45}$ ergs s^{-1}. Second, the disk axis of the source must be within smaller angles (say, $\sim 7°$) of the line of sight (see Fig. 10). The axes of BL Lacertae sources are suggested to be within $\sim 17°$ (Maraschi & Rovetti 1994), so the probability of an observed BL Lac object pointing within 7° is $\int_0^{7°} d(\cos\Theta)/\int_0^{17°} d(\cos\Theta) \sim 17\%$. This number is quite consistent with Whipple's finding ($2/15 \approx 13\%$). On the other hand, for Mrk 421 and Mrk 501, because of their lower luminosities of $\sim 10^{45}$ ergs s^{-1} (assuming isotropy), inferred from their observed flux (e.g., Mufson et al. 1984; Urry 1988), which correspond to an M_8 of 0.1 and an $\dot{M}_{26}$ of 0.1 in our calculation, the emission site and the timescale of variability are $\sim 1.3 \times 10^{-3}$ pc and ~ 1.5 days, respectively.

Now we turn to the fate of the off-axis radiation. If the high-energy γ-rays are produced isotropically at some point above the black hole, then the photons produced far from the disk axis (i.e., in the direction of large Φ angle) will produce high-energy $e^{\pm}$ pairs. These pairs will produce further photons through synchrotron radiation and/or Compton scattering, depending on the ratio of magnetic energy density, U_B, to the energy density of soft photons, $U_{\rm ph}$ (i.e., $Ra = U_B/U_{\rm ph}$). If $Ra < 1$, then Compton scattering is dominated and pair-Compton cascade (Protheroe, Mastichiadis, & Dermer 1992) will lead to a large number of lower energy photons with roughly MeV energy in the off-axis direction (see, e.g., Becker & Kafatos 1995). On the other hand, if $Ra > 1$, then these $e^{\pm}$ pairs will produce synchrotron photons whose directions are not necessarily in the direction of the $e^{\pm}$. Finally, this will result in energy accumulation in some energy band, depending on the magnetic field strength in the interaction region and the energy of the pairs. The large bump in the UV–X-ray region could result from the radiation of these off-axis $e^{\pm}$ pairs. However, a more detailed investigation is necessary. On the other hand, it is possible that the emission of high-energy γ-rays is not isotropic, due to some alignment mechanism, e.g., relativistic beaming. Furthermore, the pair production of high-energy γ-rays in the soft photon field could also lead to preferential escape of the γ-rays along the disk axis.

Note that there may exist other sources of background photons, for example, nonthermal soft photons produced by synchrotron radiation and Compton scattering of high-energy electrons (see, e.g., Lightman & Zdziarski 1987; Biermann & Strittmatter 1987; Begelman, Rudak, & Sikora 1990). Here we did not consider the contribution of the nonthermal processes of the soft photon field. On the other hand, there may be also a component of soft photons whose distribution is isotropic, consisting of scattered photons produced in the collisions of primary photons with diffuse gas or emission-line clouds; this component can be important far from the central engine (see, e.g., Dermer & Schlickeiser 1994; Sikora, Begelman, & Rees 1995; Blandford & Levinson 1995). Therefore our calculations can yield only lower limits on the optical depth of high-energy γ-rays produced in AGNs.

Finally, we remark that the inner region of the α-disk (Shakura & Sunyaev 1973) may not be stable and will become very hot. A possible model is the two-temperature model proposed by Shapiro et al. (1976), in which the temperature of electrons in the inner part is $\sim 10^9$ K, which is very important for the pair production of GeV γ-rays (Becker & Kafatos 1995), but there is very little change for the opacity of TeV γ-rays.

We thank P.-W. Kwok for his useful suggestions. This work was partially supported by an RGC grant of Hong Kong.

REFERENCES

Becker, P. A., & Kafatos, M. 1995, ApJ, 453, 83
Bednarek, W. 1993, A&A, 278, 307
Begelman, M. C., Blandford, R. D., & Rees, M. J. 1984, Rev. Mod. Phys., 56, 127
Begelman, M. C., Rudak, B., & Sikora, M. 1990, ApJ, 362, 38
Biermann, P. L., & Strittmatter, P. A. 1987, ApJ, 322, 643
Blandford, R. D. 1993, in AIP Conf. Proc. 280, Compton Gamma-Ray Observatory, ed. M. Friedlander, N. Gehrels, & D. J. Macomb (New York: AIP), 533
Blandford, R. D., & Levinson, A. 1995, ApJ, 441, 79
Bottcher, M., & Dermer, C. D. 1995, A&A, 302, 27
Carraminana, A. 1992, A&A, 264, 127
Dermer, D. C., & Schlickeiser, R. 1993, ApJ, 416, 458
———. 1994, ApJS, 90, 945
Fichtel, C. E., et al. 1994, ApJS, 94, 551
Gould, R. J., & Schréder, G. P. 1967, Phys. Rev., 155, 1408
Kerrick, A. D., et al. 1995a, ApJ, 452, 588
———. 1995b, ApJ, 438, L59
Lightman, A. P., & Zdziarski, A. A. 1987, ApJ, 319, 643
Macomb, D. J., et al. 1995, ApJ, 449, L99
Maraschi, L., & Rovetti, F. 1994, ApJ, 436, 79
Mufson, S. L., et al. 1984, ApJ, 285, 571
Protheroe, R. J., Mastichiadis, A., & Dermer, C. D. 1992, Astropart. Phys., 1, 113
Punch, M., et al. 1992, Nature, 358, 477
Quinn, J., et al. 1996, ApJ, 456, L83
Rees, M. J. 1984, A&A Rev., 22, 471
Shakura, N. I., & Sunyaev, R. A. 1973, A&A, 24, 337
Shapiro, S. L., Lightman, A. P., & Eardley, D. M. 1976, ApJ, 204, 187
Sikora, M., Begelman, M. C., & Rees, M. J. 1994, ApJ, 421, 153
Stecker, F. W., & de Jager, O. C. 1993, ApJ, 415, L71
Stecker, F. W., de Jager, O. C., & Salamon, M. H. 1992, ApJ, 390, L49
Thompson, D. J., et al. 1995, ApJS, 101, 259
von Montigny, C., et al. 1995, ApJ, 440, 525
Urry, C. M. 1988, in Multiwavelength Astrophysics, ed. F. A. Cordova (Cambridge: Cambridge Univ. Press), 279